Beam Performance

Developments and Upgrades of Storage Ring and Booster Synchrotron

Improvement of Coupling Correction

By the precise alignment of the magnets and the appropriate COD correction, at the commissioning phase of the SPring-8 storage ring, we succeeded in achieving the very small coupling of ~0.2% without correction. However, the coupling has increased over the years; thus, recently, we have corrected it and recovered the initial performance. The scheme of the coupling correction at the SPring-8 storage ring is global and is based on the perturbation theory with single resonance approximation [1-5]. The perturbation theory implies that the vertical beam size is proportional to the strength of the coupling resonance. Hence, the strengths of the skew quadrupole magnets for the coupling correction are determined so as to give the minimum of the vertical beam size [6].

After the coupling correction based on the vertical beam size response, we find that there remains the linear coupling mode in the vertical oscillation induced by the horizontal kick by the pulse bump magnets. This is because the vertical beam spread comes from the higher order coupling as well as the linear coupling. The strength of the higher order coupling may vary according to that of the linear coupling; thus, the vertical beam size is not a very suitable measure for the linear coupling correction. Then, we change the way of the coupling correction to correct the linear coupling mode in the vertical oscillation induced by the pulse bump magnet. As a result, we can almost completely eliminate the linear coupling of the beam motion at the storage ring. Figure 1 shows the process of the linear coupling correction, i.e. the change in the strength of the linear coupling mode in the vertical oscillation against the coupling driving term, where the x-axis represents the tune of the vertical oscillation, the y-axis the strength of the coupling driving term, and the z-axis the magnitude of the oscillation mode. By changing the strength of the skew quadrupole magnets appropriately, we can eliminate the linear coupling mode corresponding to the peak at the horizontal betatron tune of 0.15, as shown in Fig. 1.

To further reduce the emittance coupling, we must correct the higher order coupling as implied above. For this end, we are preparing skew sextupole magnets, which generate the higher order coupling.

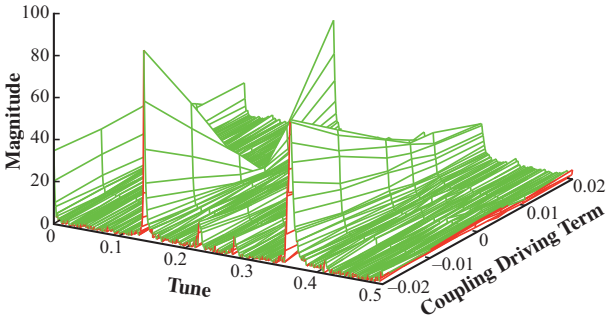

Fig. 1. Spectrum of the vertical oscillation induced by the horizontal kick of the bump magnets with the amplitude of 10 mm against the coupling driving term.

Beam Commissioning of New Lattice for Undulator Installation at LSS

The new beamline BL43LXU has been constructed in one of the long straight sections (LSSs) of the storage ring. In this beamline, small-gap in-vacuum undulators with a short period are used for generating an intense X-ray beam with very high flux and brilliance between 14.4 and 26 keV [7]. To realize a small gap of less than 6 mm, the vertical betatron function was reduced at the center of the undulator, and for this purpose, we installed two sets of quadrupole triplets in the LSS. The LSS was then divided into three subsections and, at the center of each subsection, the vertical betatron function was designed to take the minimum value of 2.5 m. By modifying the storage ring lattice locally, we inevitably lower the symmetry of the ring and this causes degradation of beam stability: the dynamic aperture and momentum acceptance become narrower, and hence the injection efficiency will be lower and the beam lifetime will be shorter. As discussed in Refs. [6,8], however, we can solve this problem and recover the beam stability by combining the schemes of betatron-phase matching, local chromaticity correction and mutual cancellation of nonlinear kicks due to sextupoles. Simulation results show that the dynamic aperture can be kept large even after modifying the lattice.

After installing the quadrupoles in March 2011, we carried out beam tuning of the new lattice and checked its performance. Machine parameters, such as dispersion and betatron functions, beam size, coupling ratio, injection efficiency and beam lifetime, were measured and compared with the design value and/or the value of the original lattice before modification. As examples of measured machine parameters, we show the horizontal and vertical betatron functions in the modified section in Fig. 2.

These were obtained by response matrix analysis, and we see a good agreement between the measured and design values. At present, the overall distortions of the betatron function along the ring are 2.3% in the horizontal direction and 2.4% in the vertical direction. These distortions were corrected with 49 auxiliary power supplies to quadrupoles, and we will soon make further corrections to suppress the distortions to less than 2%.

From the results of beam tests, we concluded that the beam performance of the new lattice is as good as the original one, and from September 2011, the new lattice has been dedicated to user operation. One undulator has been installed in the middle subsection and the other two undulators are planned to be installed within a few years. The minimum gap allowed in the user operation is 5.8 mm, while from a point of view of beam dynamics, the gap of 5.2 mm is the acceptable minimum.

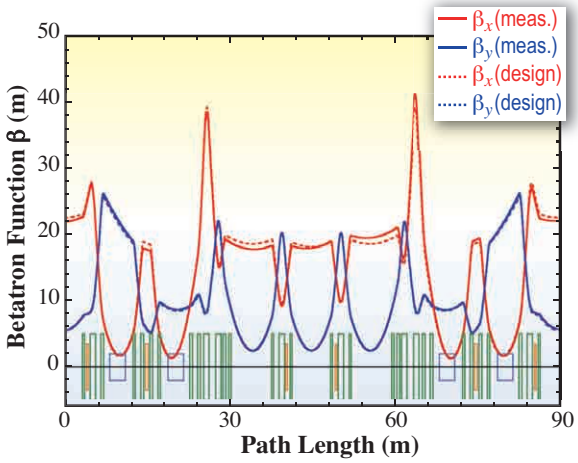

Fig. 2. Betatron function in the modified section including LSS. The solid curves are the horizontal (β_x) and vertical (β_y) betatron functions obtained by response matrix analysis and the dashed curves are the design values. Also shown in the figure is the magnet arrangement (blue: bending magnets, green: quadrupole magnets, orange: sextupole magnets).

Optimization of Lower Emittance Optics for SPring-8 Storage Ring

A design work to modify the present SPring-8 storage ring optics is in progress to provide photon beams with higher brilliance and flux density to current users. The new optics with the lower natural emittance of 2.4 nm·rad than the present optics (3.4 nm·rad) has been designed. It is noted that, in this optics, magnetic positions and polarities are maintained and magnetic fields are optimized within the specifications, so that the optics can easily be changed from the present optics without any shutdown time. The new optics has experimentally been examined at the machine study run. The machine conditions, such as the injection efficiency, the bump orbit for the injection and the vertical dispersion function, have been tuned, and the photon beam performance has been observed by utilizing the accelerator diagnostics beamlines I (BL38B2) and II (BL05SS).

The emittance was determined by measuring the electron beam size with the X-ray beam imager at the diagnostics beamline I, and by using the lattice functions estimated by response matrix analysis. The resulting value of the horizontal emittance shows a good agreement with the design value. The vertical emittance was found to be larger than that of the present optics (present: 12.55 pm·rad, new: 31.46 pm·rad), though the vertical dispersion function and the linear coupling resonance were corrected by the skew quadrupole magnets. From the results of the measurement of the betatron oscillation spectrum, it seems that the vertical emittance growth is caused by the coupling resonance induced by skew sextupole magnetic fields. We will suppress the vertical emittance by optimizing the betatron tunes and by avoiding the resonance.

The flux density of 10 keV photons from the insertion device (ID) was measured at the diagnostics beamline II. The flux density of the new optics was 1.3 times higher than that of the present optics (see Fig. 3), and this result is consistent with the theoretical calculation by SPECTRA [9], in which the above-determined emittances and estimated lattice functions are assumed. This also suggests a possibility that if we operate the ring at a lower energy of 7 GeV to save electric power, we can use the new optics to recover the photon beam performance of ID beamlines to the same level as that of the present optics at 8 GeV.

After optimizing the machine conditions e.g., the vertical emittance, the top-up injection efficiency, and the beam lifetime and verifying the photon beam performance at the beamlines, the new optics will be applied to the user operation.

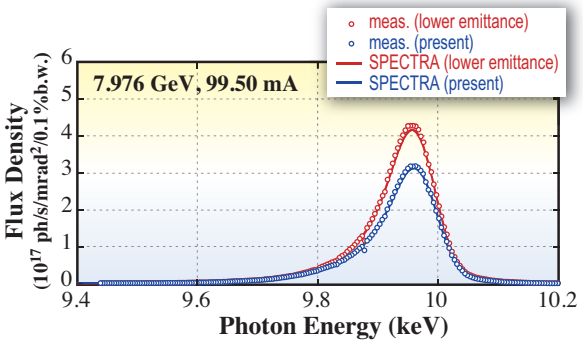

Fig. 3. Flux density of 10 keV photons for ID measured at the diagnostics beamline II (BL05SS).

Short X-ray Pulse Generation with Vertical Kicker

There are a number of requests for a short-pulsed X-ray with a pulse width of around 1 ps for a pump-probe experiment. For these requests, from 2008, we have developed a scheme of short pulsed X-ray generation with a vertical kicker in the storage ring [10,11].

A vertical kick induces a beam head-tail oscillation and finally a vertical beam tilt by synchrotron-betatron coupling due to a non-zero chromaticity [12]. By slitting a radiated X-ray pulse coming from the tilted electron bunch, we can obtain a short-pulsed radiation. Compared with other complex schemes for generating short X-ray pulses, this scheme utilizing a small vertical beam has advantages of the simplest system and the easiest handling; only a small vertical kicker and a trigger timing system are necessary. Although the radiation flux is reduced by light slitting, short-pulsed X-ray can be supplied to all the beamlines by just installing a 30-cm-long vertical kicker.

The following are the two key technical issues in obtaining short X-ray pulses: 1) development of a fast and strong kicker to realize a large tilted electron bunch and 2) understanding the correlation between the storage ring accelerator parameters, such as chromaticity, betatron tune and beam tilt, to obtain a reproducible condition that provides a suitably large beam tilt for slitting.

For the first issue, we have been developing fast-pulsed power supply systems for the vertical kicker. The power of the vertical kicker increased with the progress of high-voltage resistant switching devices: from a 157-A-amplitude, 2.6-μs-width pulse with a test-type kicker system by the year 2009, through a 338 A-amplitude, 2.5-μs-width pulse with a prototype model in 2009-2010, to a 641-A-amplitude, 1.8-μs-width pulse with a developed model, as shown in Table 1. In addition to the amplitude and width improvements, the repetition rate of the pulse increased to 200 Hz.

A high-voltage power supply controls the vertical kick power. The voltage range from 200 to 950 V corresponds to the 0.9 to 4.2 mm vertical oscillation amplitude range. The developed system can generate a maximum vertical kick of about 0.15 mrad and a pulse width as small as 2.4 μs with 200 Hz repetition rate. Figure 4 shows the excitation of the vertical beam oscillation as a function of vertical kicker power. With this system, we successfully observed a longitudinal bunch profile that tilted from 83 to 378 mrad as a function of vertical kick power, as shown in Fig. 5, by a visible-light streak camera measurement. We defined the good tilt (GT) as the bunch center located on the right axis, and the tilt angle was maximum while keeping the bunch shape aligned on a straight line. The bunch shape projected on the s-y plane twisted and deviated from a straight line when the bunch came closer to the maximum tilting angle, where s denotes the beam axis and y the vertical direction.

Table 1. The vertical kicker power progress

Item	Test model ~2009.3	Prototype model 2009.4~2010.3	Developed model 2010.4~
Max. Cur.	157 A/coil/2.9 mT	338 A/coil, 6.9 mT	641 A (2.4 μs), 13.1 mT
Pulse width	2.6 μs	2.5 μs	1.8 μs~3.6 μs
Repetition	1 Hz	1 Hz	200 Hz
No. of FET	2 parallel @ 400 V	4 parallel @ 600 V	6 parallel @ 1 kV

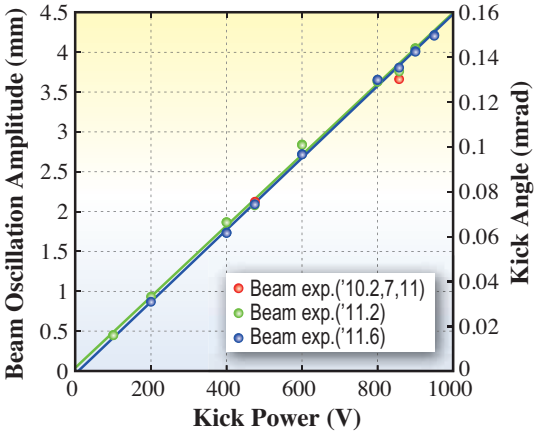

Fig. 4. Excited vertical oscillation amplitude by vertical kicker. The different color marks correspond to the results of experiments performed in different dates.

For the second issue, we have been studying the storage ring parameters to obtain the optimum tilting condition for the short-pulsed radiation by cutting out with vertical slits. By introducing the quantitative evaluation method using the measured data with a visible-light streak camera, we understood the following correlations between the beam tilt and accelerator parameters; the data used for evaluation were the beam tilt angle, the vertical shift from the light axis, and the beam tilt shape. i) The vertical chromaticity should be set to a low value of around 2 to induce the linear beam tilt, ii) there is an optimum turn number at which the linear-shape maximum beam tilt on the light axis depending on the kick power and vertical tune, iii) the reproducibility of the kick power, vertical chromaticity, and vertical tune values were required to be less than 1%, 0.1, and 0.01, respectively.

We confirmed the reproducibility of the above conditions. The X-ray pulse of 675 fs was expected by assuming the absence of emittance growth, with an

achieved good tilt angle of 266 mrad (GT) with 800 V kick power, with good reproducibility. The pulse width was estimated from the tilt angle observed in the visible-light streak camera measurement. We will confirm this by a measurement utilizing an X-ray streak camera with the actual cutting out of the radiation by vertical slits.

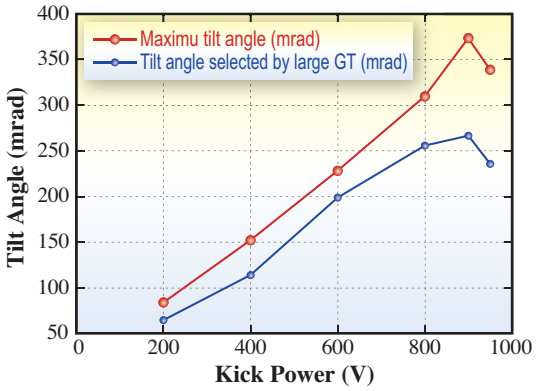

Fig. 5. Induced beam bunch tilts by vertical kicks. The red point shows the maximum tilt angle and the blue point shows the maximum tilt angle when the center of the bunch locates on the light axis keeping the linear bunch shape in the s-y plane.

Development of Bunch-by-Bunch Feedback System

The hybrid filling composed of a high-current singlet bunch with 6 mA/bunch and a bunch train with low bunch current, as shown in Fig. 6, was achieved with the sufficient stability and performance for user operation, and test operations with beamline staff members were performed.

At such filling, the horizontal and vertical beam instabilities for singlets, e.g., mode-coupling single-bunch instability, and for trains, e.g., multi-bunch instabilities by the resistive wall of IDs and cavity higher order modes, are simultaneously successfully suppressed by bunch-by-bunch feedback. The key component that can be used to achieve this is the newly developed bunch current sensitive automatic attenuator [13] placed at the front-end of the feedback [14] (Fig. 7). The feedback detects the position using the signal from the beam position monitor (BPM), calculates the kick necessary to damp the oscillation, and then drives the kicker with it. However, the BPM signal is proportional to the position and current of the bunch; therefore, its level for a high-current singlet, which is ~100 times larger than that of the trains, is so high that it leads the feedback to saturation if the BPM signal is directly fed to the feedback. The automatic

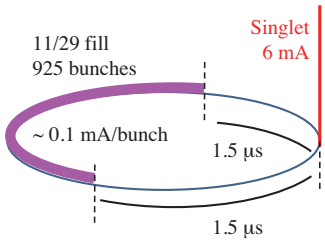

Fig. 6. Hybrid filling with high current singlet.

attenuator detects the bunch current and controls the attenuators bunch-by-bunch base to reduce the large BPM signal level of the singlets to be controllable. This simultaneous suppression of single-bunch and multi-bunch instabilities under the high contrast of the bunch current is, to the best of knowledge, the first in the world.

Also, the very fast growth of the single bunch instability (mode-coupling instability) is suppressed even under the large horizontal oscillation excited by the injection bump formation with the developed high-efficiency horizontal kickers.

Currently, the range of the filling of the trains is limited by the kicker strength, and the bunch current is also assumed to be limited. The installation of the newly developed high-efficiency high-power kicker scheduled in March 2012 is expected to increase the range of the filling and to increase the bunch current to 10 mA/bunch.

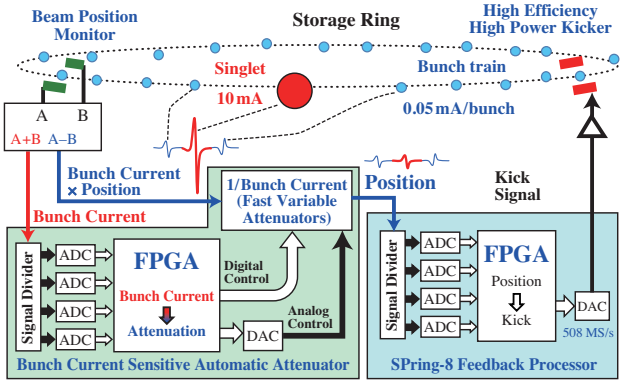

Fig. 7. Bunch-by-bunch feedback with bunch current sensitive automatic attenuator.

Development of Accelerator Diagnostics Beamlines

The fluctuation analysis of the power of the synchrotron radiation pulse [15] is a promising method for the length measurement of sub-ps short bunches. When the radiation pulse has a coherence length comparable to the source bunch length, its pulse-to-pulse intensity fluctuation is sensitive to the bunch

length. The required spectral bandwidth to obtain a sufficient small coherence length for sub-ps short bunches is moderate compared with those for long bunches, making the method advantageous the length measurement of short bunches. The feasibility of the fluctuation method was studied at the diagnostics beamline I (BL38B2) by observing visible synchrotron light pulse from a dipole magnet. An interferometric filter with a bandwidth of 1 nm (FWHM) and a silicon avalanche photodiode (APD) module with an embedded amplifier were used. To reduce the number of transverse coherent modes contributing to signal fluctuations, the angular acceptance was limited by a 4-jaw slit in front of the focusing lens to the APD. The detected signals were analyzed using a fast digital oscilloscope. Figure 8 shows an example of a set of intensity histograms for 5000 measurements of a single bunch beam in an experimental 7 GeV operation. The bunch current and RF voltage were 0.2 mA and 18 MV, respectively. The fluctuation ΔI/I was calculated by subtracting the fluctuation of the baseline originating from electronic noise. The bunch length deduced by further taking into account the contributions of photon shot noise and transverse beam emittance was 11.3 ps (r.m.s.), which is consistent with that of 10.8 ps measured simultaneously with a visible light streak camera. The reduction of fluctuation for long bunches obtained by increasing the bunch current was also observed. Further studies of turn-by-turn measurement are planned by using a single-shot visible light monochromator.

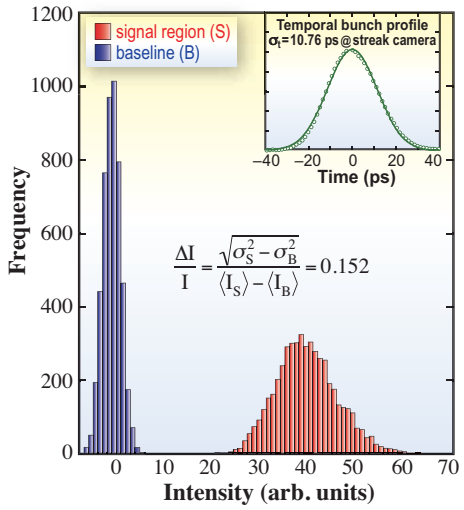

Fig. 8. Example of a set of histograms of intensities in the signal region (red) and the baseline (blue) obtained by integrating oscilloscope traces for 5000 measurements of a single bunch beam. The fluctuation of the detected power of synchrotron radiation pulse ΔI/I is calculated by subtracting the fluctuation of the baseline. The inset shows a temporal bunch profile measured simultaneously with a visible light streak camera (circles) and a fitted Gaussian curve (line).

Increasing Cooling Power of Storage Ring RF Cavities

To increase the beam lifetime, it was desired to apply a higher acceleration voltage to the RF cavities. However, the cooling ability of the cavities was the limiting factor against increasing the acceleration voltage. When the higher acceleration voltage is applied to the cavities, the wall loss of the cavities increases, which requires the increase in the cooling ability of the cavities.

To improve the cooling ability, the heat exchangers with an exchange capacity of 400 kW were replaced with those with an exchange capacity of 600 kW in March 2011. As a result, the acceleration voltage of 19.1 MV became possible, while that of 16 MV was the largest before the replacement. A study was conducted to ensure temperature stability during the 19 MV operation. The acceleration voltage applied to the cavities was gradually increased to 19 MV while observing the temperature change. The cooling water temperatures at the cavity inputs were kept constant within 0.01°C around the 30°C set value up to the 19 MV operation.

As for the configuration of the RF system, there are four RF stations in the storage ring, which are named A, B, C and D stations. In each RF station, a 1 MW klystron delivers the RF power to 8 single cell cavities. The exception is the A station, where 2 klystrons are placed and each supplies the power to 4 cavities. The acceleration voltage is the sum of the voltages evenly supplied by all the four stations. For the 16 MV operation, each station supplies 4 MV, while for the 19.1 MV operation, each station supplies 4.8 MV. If the voltages of three stations are summed, the total voltage is 12 MV before the improvement of the cooling system, while it is 14.4 MV after the improvement. With the 14.4 MV operation, the reduction in beam lifetime is tolerable for the 100 mA user operation. Before the improvement, only about 70 mA could be stored in the storage ring with three-station feeding. Therefore, one of the advantages of increasing the cooling ability is the possibility of maintaining the beam current, even if one of the four RF stations fails. Another advantageous effect of the higher acceleration voltage is a longer Touschek lifetime for the same amount of a single bunch current, or larger single bunch current for the same Touschek lifetime, which can provide a larger number of options in filling patterns in the storage ring.

On the other hand, in spite of the improvement of the higher RF voltage ability, the actual operation has been performed with 16 MV or 14.4 MV acceleration voltage, since the electricity-saving requirement was issued. The cause was the lack of electricity due to

from the shutdown of most of the nuclear power plants in Japan after the disastrous earthquake on March 11, 2011 and the successive occurrence of accidents in the Fukushima Dai-ichi nuclear power plant. We expect that the situation of electricity supply will get better and we will have the full benefit of the improvement of the RF cavity cooling system in the near future.

Developments and Upgrades of Linac

Research and Development of Beam Position Monitors for Second-Order Moment Measurement

We are installing new BPMs at the SPring-8 linac, which measure the transverse second-order moments of electron beams, as an enhancement of non-destructive beam diagnosis during top-up injection.

To design the system, we first constructed the comprehensive theory for BPMs [16]. This theory presents an analysis and design method for a stripline-type BPM that detects the multipole moments of a charged particle beam. A numerical analysis based on the finite difference method was also carried out to calculate the electric fields in a BPM.

According to this design method, we have developed six-electrode BPMs with circular (Fig. 9) and quasi-elliptical cross sections for non-dispersive and dispersive sections, respectively. The results of the numerical calculations show that the second-order moment can be detected for beam sizes >0.42 mm (circular) and >0.55 mm (quasi-elliptical). The actual beam sizes are >0.5 mm in the non-dispersive sections and >0.75 mm in the dispersive sections, that is, they are sufficiently large to enable accurate measurements of the second-order moments using these BPMs.

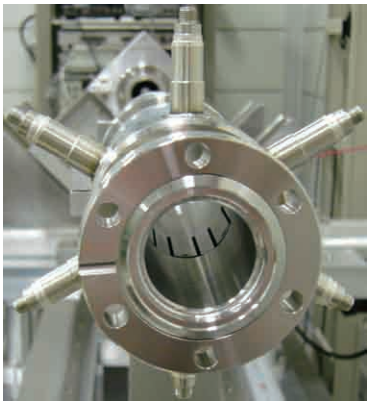

Fig. 9. Six-electrode BPM with circular cross section.

The measurement of a second-order moment requires a good measurement accuracy of about 10^{-4}. Therefore, we developed a low-noise signal processor (Fig. 10) with six channels. The previous signal processor with four channels contained sample-and-hold circuits that generate large sample-and-hold noises. The new signal processor, however, does not employ any sample-and-hold circuit; thus, fast and low-noise analog-to-digital converters (LTC2393, LINEAR TECHNOLOGY) directly acquire signals from the peak-hold circuits. The dynamic range of the signal processor is finally increased to 80 dB, and the maximum signal-to-noise (S/N) ratio is 80 dB.

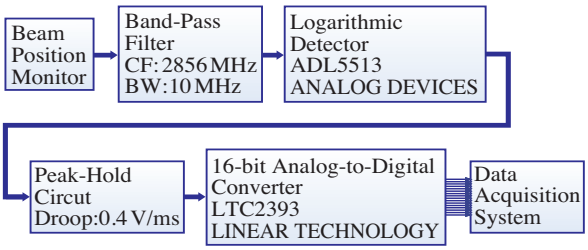

Fig. 10. Block diagram of signal processor (one of six channels).

Haruo Ohkuma, Shigeki Sasaki and Hirofumi Hanaki

SPring-8/JASRI

E-mail: ohkuma@spring8.or.jp

References

[1] G. Guignard: Phys. Rev. E **51** (1995) 6104.
[2] M. Takao: Proc. of EPAC'06, Edinburgh, UK, p.1975.
[3] M. Takao: Phys. Rev. ST Accel. Beams **9** (2006) 084002.
[4] M. Masaki *et al.*: Proc. of EPAC'08, Genoa, Italy, p.3035.
[5] M. Masaki *et al.*: Phys. Rev. ST Accel. Beams **12** (2009) 024002.
[6] SPring-8 Research Frontiers 2009, p.153.
[7] A. Baron: SPring-8 Information **15** (2010) p.14.
[8] K. Soutome *et al.*: Proc. of IPAC'10, Kyoto, Japan, p.4497.
[9] T. Tanaka and H. Kitamura: SPECRA code ver. 9.02 (2012).
[10] C. Mitsuda *et al.*: Proc. of SRI'09, Melbourne, Australia, AIP Conference Proc. 1234, p.193.
[11] C. Mitsuda *et al.*: Proc. of PAC'09, Vancouver, Canada, p.1171.
[12] W. Guo *et al.*: Phys. Rev. ST Accel. Beams **10** (2007) 020701.
[13] K. Kobayashi *et al.*: Proc. of ICALEPCS 2009, Kobe, Japan, p.659.
[14] T. Nakamura *et al.*: Proc. of ICALEPCS 2005, Geneva, Switzerland, PO2.022-2.
[15] M. S. Zolotorev and G. V. Stupakov: SLAC-PUB-7132, March 1996.
[16] K. Yanagida *et al.*: Phys. Rev. ST Accel. Beams **15** (2012) 012801.